ELSEVIER

Earth and Planetary Science Letters 182 (2000) 137–156

EPSL

www.elsevier.com/locate/epsl

Cosmic markers, $^{40}Ar/^{39}Ar$ dating and paleomagnetism of the KT sections in the Anjar Area of the Deccan large igneous province

V. Courtillot [a,*], Y. Gallet [a], R. Rocchia [b], G. Féraud [c], E. Robin [b], C. Hofmann [a], N. Bhandari [d], Z.G. Ghevariya [e]

[a] *Institut de Physique du Globe and Université Paris 7, 4 Place Jussieu, 75252 Paris Cedex 05, France*
[b] *Laboratoire des Sciences du Climat et de l'Environnement (CEA-CNRS), Domaine du CNRS, Avenue de la Terrasse, 91198 Gif-sur-Yvette Cedex, France*
[c] *UMR Géosciences Azur, CNRS-UNSA, Parc Valrose, 06108 Nice Cedex 02, France*
[d] *Physical Research Laboratory, Navrangpura, Ahmedabad 380009, India*
[e] *Geological Survey of India, Gandhinagar 382043, India*

Received 20 April 2000; accepted 9 August 2000

Abstract

Bhandari et al. [Bhandari et al., Geophys. Res. Lett. 22 (1995) 433–436; Bhandari et al., Geol. Soc. Am. Spec. Paper 307 (1996) 417–424] reported the discovery of iridium-bearing sediments sandwiched between basalt flows in the Anjar area (Kutch province, India). They concluded that the signature of the K/T impact had been recorded and that onset of volcanism in the Deccan traps preceded the K/T boundary, excluding the possibility of a causal connection. This paper reports complementary analyses of Anjar outcrops by a joint Indo–French team, where we focused on cosmic markers (iridium and spinels) in the intertrappean sediments and $^{40}Ar/^{39}Ar$ dating and paleomagnetism of the lava flows. Anomalous Ir concentrations (up to 0.4 ng/g) are confirmed, with up to three thin and patchy enriched layers which cannot be traced throughout the exposed sections. Despite careful search, no Ni-rich spinels were found. Eight basalt samples provided $^{40}Ar/^{39}Ar$ results, four on plagioclase bulk samples, four on whole rocks. Spectra for whole rocks all indicate some amount of disturbance, and ages based on plagioclase bulk samples seem to be consistently more reliable [Hofmann et al., Earth Planet. Sci. Lett. 180 (2000) 13–28]. The three flows underlying the Ir-bearing sediments are dated at $\sim$66.5 Ma, and two overlying flows at $\sim$65 Ma. Magnetic analyses (both thermal and by alternating fields) uncovered clear reversed primary components in the upper flows, and more disturbed normal components in the lower flows, with evidence for an additional reversed component. There are reports [Bajpai, Geol. Soc. India Mem. 37 (1996) 313–319; Bajpai, J. Geol. Soc. London 157 (2000) 257–260] that the intertrappean sediments contain uppermost Maastrichtian dinosaur and ostracod remains above the uppermost Ir-bearing level, and may not be mechanically disturbed. We propose the following scenario to interpret these multiple field and analytical observations. Deccan trap volcanism started within uppermost Maastrichtian normal chron C30N at $\sim$66.5–67 Ma in the Anjar area. Volcanism then stopped at least locally, and lacustrine sediments were deposited over a period that could be in the order of 1–2 Ma. The K/T bolide impact was recorded as a deposit of Ir, and possibly (though not necessarily) spinels. Volcanism

* Corresponding author. Tel.: +33-1-4427-3908; Fax: +33-1-4427-7463; E-mail: courtil@ipgp.jussieu.fr

0012-821X/00/$ – see front matter
PII: S0012-821X(00)00238-7

resumed shortly after the K/T boundary, within reversed chron C29R, as witnessed by the three reversely magnetised overlying basalt flows dated ~65 Ma. This was responsible for erosion and destruction of part of the uppermost sediments (including spinels if there were any) and heterogeneous and non-uniform redeposition of Ir at a number of underlying sedimentary levels. This was also responsible for the partial remagnetisation of the underlying flows. These findings generally confirm and complement those of Bhandari et al. [Bhandari et al., Geophys. Res. Lett. 22 (1995) 433–436; Bhandari et al., Geol. Soc. Am. Spec. Paper 307 (1996) 417–424], and are compatible with the occurrence of the K/T impact at the paleontological K/T boundary, and of Deccan trap volcanism straddling the boundary and starting before the impact. Anjar provides evidence for minor volcanism somewhat earlier than suggested by some authors, though still within normal chron C30N. There is no indication contradicting the view that the bulk of Deccan trap volcanism occurred over only three chrons (C30N, C29R, C29N) [Courtillot, Evolutionary Catastrophes: the Science of Mass Extinctions, Cambridge University Press, 1999; Courtillot et al., Earth Planet. Sci. Lett. 80 (1986) 361–374; Vandamme et al., Rev. Geophys. 29 (1991) 159–190].

Keywords: Deccan Traps; volcanism; impacts; iridium; paleomagnetism

1. Introduction

In the two decades following the discovery of an iridium layer in sedimentary sections containing the Cretaceous–Tertiary boundary [9], two main scenarios, one involving an asteroid or cometary impact, the other a massive volcanic eruption, have been suggested as the cause of the mass extinction. Work on both the Deccan traps of India and the Chicxulub impact crater in Mexico has confirmed that both 'catastrophic' events actually occurred at the same time, though on different time scales, and must be taken into account in any quantitative model of the evolutionary turnover (for overviews see, for example, [6,10]).

A major step in establishing the occurrence and relative timings of impact and volcanism has been the identification by Bhandari et al. [1,2] of an iridium-enriched layer in intertrappean sediments within the thin series of Deccan flows in the Anjar area (Kutch province, western India). Bhandari et al. [1] measured concentrations of Ir and Os 15 times higher than in adjacent sediments and two orders of magnitude higher than the underlying basalts. Based on chemical and stratigraphic criteria, they concluded that a limonite layer did correspond to the fallout ejecta of the KTB bolide impact. They also concluded that volcanism was already active when the impact occurred and therefore could not have been triggered by it.

These results were deemed most important and a joint Indo–French team of geochemists and geophysicists returned to the Anjar region in April 1995 for complementary sampling. $^{40}Ar/^{39}Ar$ dating of the flows and further chemical analyses performed in India were reported, respectively, by Venkatesan et al. [11] and by Shukla et al. [12]. Preliminary $^{40}Ar/^{39}Ar$ and paleomagnetic results obtained in France were reported by Hofmann [13]. These, together with analysis of cosmic markers (iridium and Ni-rich spinels) are the focus of the present paper. Overall, they tend to confirm the original findings of Bhandari et al., but uncover new complexities and remaining uncertainties, leading to at least two possible scenarios of volcanism at Anjar.

2. Background and sampling

The sampling location near Anjar (20.06°N, 70.05°E; Fig. 1) is only about 30 km^2 in area. Because of the flat-lying volcanic flows and intertrappean layers, and overall subdued topography, fresh sites were found only in quarries or along small rivers. Previous geological mapping by Ghevariya [14] indicated a sequence of seven basaltic flows (roman numbers I to VII), as reported by Bhandari et al. [1]. However, only a single, generally flat-lying flow could be observed at any single outcrop (site). Recently, Shukla et al. [12] have revised the stratigraphy to nine flows (arabic numbers F1 to F9), although the map in Fig. 1 (after [14]) displays only the original seven. Table 1 gives the correspondence between the numbering systems used by successive authors, and lists

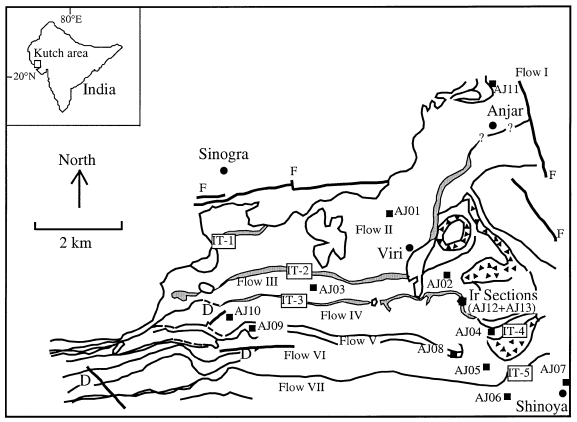

Fig. 1. Simplified geological map of basalt flows (see text and Table 1) and intertraps (IT1 to 3) in Anjar [12,14]. IT = intertrappean sedimentary level; D = dyke; F = normal fault. Sites sampled in flows for paleomagnetism and age determination (AJ with numbers see Table 1) and the site of intertrappean sediment sampling (in IT3) are shown as squares and a star, respectively.

the sites collected for $^{40}Ar/^{39}Ar$ or paleomagnetic analysis. There is no stratigraphic problem with the three flows underlying the Ir-rich sediments (flows F1 to F3, sites AJ11 and AJ01 to 03). Sites AJ04 and AJ10 were originally taken to be part of flow IV above the sediments, although their textures and morphologies were quite different from one another. In the later paper by Shukla et al. [7], site AJ10 is now considered as part of an independent flow (F5), overlying F4 (to which AJ04 belongs). Furthermore, sites AJ08 and AJ09 were originally thought to be part of a single flow (V) and are now considered separate (F6 and F7). As a result, the two upper flows VI and VII have been renamed F8 and F9. This assignment problem, and the map, underscore the fact that assessing the lateral continuity of the flows is far from straightforward. This will be kept in mind in the final discussion (we will in general use the latest, F1 to F9, nomenclature).

Classical chemical analyses by Shukla et al. [12] indicate that all flows (F1 to F8) are alkali basalts resembling ocean island basalts, except the topmost flow F9 which is tholeitic. Many trace element ratios are similar to the Réunion Island basalts and consistent with a plume origin of the traps (e.g. [7]). Shukla et al. [12] quote four plateau and isochron ages for flows F1, F2, F3 and F9 from Venkatesan et al. [11] and three integrated ages for F4, F6 and F8 from Venkatesan and Pande (1998, private communication). All are for whole rocks: F3 to F8 are dated approximately as 65 Ma old (hence very close to and consistent with a K/T age), whereas flow F1 appears to be close to 69 Ma and flow F9 to 61 Ma, indicating a possible span of 8 Ma for volcanism in Anjar.

During the April 1995 sampling trip, samples were collected for paleomagnetism from all flows except F8 (VI; altered, displaced boulders) and for $^{40}Ar/^{39}Ar$ dating from all flows except F5 and F7. Because basalts often appeared somewhat altered in outcrop, we sometimes tried to sample

Table 1
Correspondence between lava flow identification following Shukla et al. [12] (first column), Ghevariya [13] (second column), sampled site code AJ (third column), and indication of an available paleomagnetic and $^{40}Ar/^{39}Ar$ age result

Lava flows		Site number	Magnetic polarity	Ar/Ar dating
Ref. [12]	Ref. [13]			
VII	F9	AJ06	R	yes
VI	F8	AJ05	n.a.	yes
V	F7	AJ09	N/R	n.a.
V	F6	AJ08	R	yes
IV	F5	AJ10	N	n.a.
IV	F4	AJ04	R	yes
III	F3	AJ02, AJ03	N/R	yes
II	F2	AJ01	N/R	yes
I	F1	AJ11	N/R	yes

N = primary normal polarity, R = primary reversed polarity, n.a. = not available

the same flow in two distinct locations. This was the case for flows III (AJ02, AJ03), IV (AJ04, AJ10) and V (AJ 08, AJ09). But since then, flows IV and V have been reinterpreted as being more complex, and only flow III (F3) apparently has two distinct sites.

As far as sediments are concerned, 25 samples were collected for iridium and spinel analysis

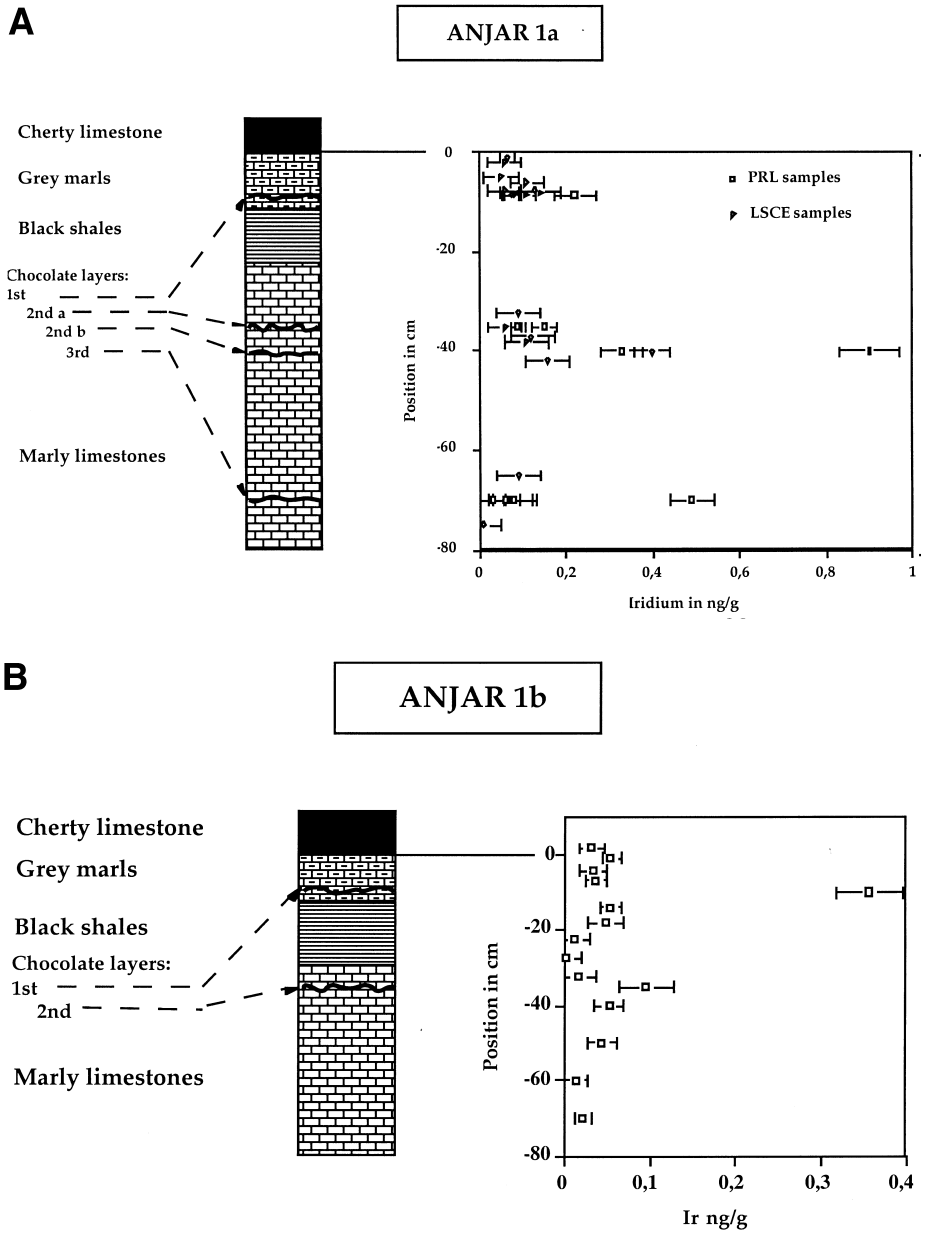

Fig. 2. Iridium measurements (in ng g^{-1}) in three sections of intertrappean sediments IT3 at three nearby locations (all within the site shown as a star in Fig. 1). In each case a simplified geological section with rock types and sedimentary observations, and an iridium profile are shown. (A) Anjar 1a, (B) Anjar 1b and (C) Anjar 2. The samples measured in the Physical Research Laboratory in Ahmedabad, India, are marked PRL; those measured in the Laboratoire des Sciences du Climat et de l'Environnement in Gif-sur-Yvette, France, are marked SCE.

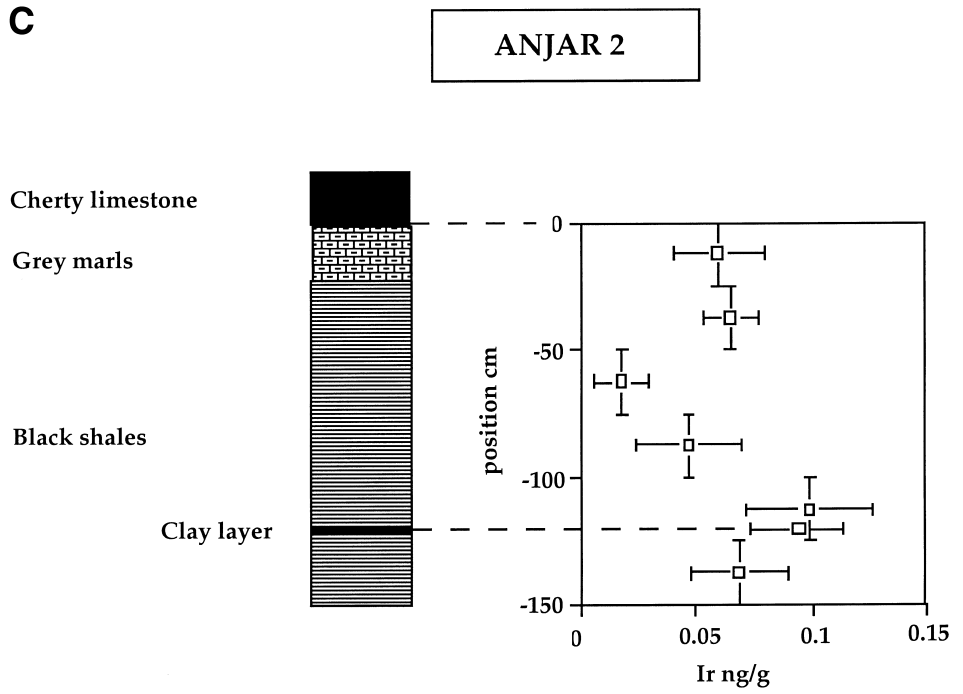

Fig. 2 (*continued*).

from the site previously explored and analysed by Bhandari et al. [1,2], called Anjar I in the following (BGI in Shukla et al. [12]). Fifteen samples were collected where the three chocolate-colour layers were clearly visible (Anjar Ia). Because the second layer seemed to consist of two sublayers, another section was sampled (15 samples), 5 m to the east, where only one rust-coloured layer could be optically identified (Anjar Ib). Ten samples from a previous collection of Anjar I were also provided by N.B. to R.R. In addition, six samples were collected at another nearby yet different outcrop (Anjar II), a few hundred meters north-west of Anjar I. Anjar II should correspond stratigraphically to site BG4 or BG5 in Shukla et al. [12]. This section differs from Anjar I: its 1.6 m thickness corresponds to the 0.5 m thick grey shales located below a crusty limestone bed at Anjar I. Each 'sample' actually corresponds to 0.2–0.3 m of sediment, not to a more discrete sampling. Two sites (AJ12 and AJ13) were sampled for paleomagnetism at Anjar I (respectively, below and above the three Ir-rich layers of Bhandari et al. [1]).

We first report the search for cosmic markers in the intertrappean sediments, then results from $^{40}Ar/^{39}Ar$ dating, then paleomagnetic analysis of the lava flows, all these being discussed together in a final section.

3. Cosmic markers

The purpose of this part of the study was to identify Ni-rich spinel, a mineral derived from the oxidation of meteoritic material layer [15] which is usually found in the K/T boundary clay layer [16–19]. The multiple Ir-rich levels identified in Anjar [1] raise questions about the conditions of sedimentation and/or about the possible occurrence of multiple impacts at the end of the Cretaceous. The identification of Ni-rich spinel crystals in one or several of the Anjar Ir levels would help to understand the formation conditions of this unusual section. We selected those samples most enriched in Ir. All samples with concentrations higher than 0.1 ng g^{-1} were then analysed for Ni-rich spinel.

3.1. Iridium

Iridium concentrations were measured by instrumental neutron activation analysis of whole rock samples. Samples, about 100 mg each, housed and sealed in pure silica vials, were irradiated for 3–4 h in the 10^{14} n cm^{-2} s^{-1} neutron beam of the Osiris reactor (Pierre Süe Laboratory, Saclay). Ir was counted for a few hours with a coincidence spectrometer (see [20,21] for a description of the method) detecting the coincidence of 316–468 keV γ-ray lines resulting from the radioactive decay of ^{192}Ir. Two Ir standards were used: fragments ($\sim$0.050 mg) of the Negrillo iron meteorite (a very homogeneous meteorite calibrated in the Orsay-Gif laboratory) and small pieces ($\cong$0.2 mg) of an Ir–Al alloy with 5.2 ppm of Ir. The detection limit is around 25 pg g^{-1}. Two basalt samples from flows F3 and F4 were analysed with slightly improved sensitivity.

Data from Anjar 1a are plotted on Fig. 2a. One can first note that the background value is high, around 50–100 pg g^{-1}. Three small maxima are observed in chocolate-coloured limonitic layers 1, 2 bis and 3. It is worth noting that the highest concentrations are found in the samples provided by N.B. In Anjar Ib (Fig. 2b), we find a first maximum 10 cm below the base of the chert bed, possibly the horizontal equivalent of the first chocolate-coloured layer of Anjar Ia (but here the colour is light grey). The rust-coloured layer (35 cm below the base of the chert bed) also shows a very small overconcentration. The correspondence with layers 2, 2 bis or 3 is uncertain. In Anjar II (Fig. 2c), two samples have low but significant Ir concentrations. In the basalt samples of flows F3 and F4, Ir concentrations are lower than 25 pg g^{-1}.

Our data confirm the existence of several Ir-enriched levels in the intertrappean layers [1]. We note however that these levels cannot be regarded as continuous horizons: they are not well defined and locally display some splitting. Such small scale heterogeneities are likely to explain the differences between the concentrations found in our samples (LSCE samples) and in those previously collected by N. Bhandari (PRL samples). PRL samples were especially selected for their dark chocolate colour. In contrast, LSCE samples were neither selected in the field nor in the laboratory. They are bulk samples representing some horizontal average of the so-called chocolate layers. In addition they might have been contaminated by the material from adjacent layers. The differences between concentrations in PRL samples analyzed at PRL, on one hand, and at LSCE, on the other, are probably due to a similar reason. PRL samples analyzed at LSCE were collected by PRL but ground and homogenized at LSCE without preselection for their dark colour. Under such conditions it is not surprising that the measured Ir concentrations in PRL samples analyzed at LSCE (for instance: 0.9 ng/g in the second chocolate layer) are higher than in LSCE samples (0.4 ng/g in the same layer), and that the Ir concentrations in PRL samples appear still higher when prepared and analyzed at PRL (1.2–1.6 ng/g). The multiple Ir-enriched levels together with the strong horizontal differences between Anjar 1a and Anjar 1b, separated by only a few meters, suggest that sediments were severely reworked.

3.2. Ni-rich spinel

Ni-rich spinel is a strongly magnetic mineral, which can be easily extracted from a liquid phase with an electro-magnet. Each sample was selected from well-ground and homogenised sediment. The sample weights were in the range 500–1000 mg. After dissolution of the carbonate fraction, using 10% hydrochloric acid, the residue was circulated in a closed-loop funnel, activated by a peristaltic pump. Magnetic particles were collected in a glass tube placed in the gap of a magnetic separator. The separator was run for 20–30 min to ensure that all magnetic particles would be collected. The funnel was then rinsed with water. The magnetic separator was switched off and the particles arrested in the magnet gap were washed out with alcohol and recovered on a 0.4 μm Nucleopore filter. The collection efficiency of the system for magnetic particles such as Ni-rich spinel was higher then 95%. Crystals larger than 1 μm were counted and sorted according to size and composition, using a JEOL 840 scanning electron micro-

Table 2
Detailed ^{40}Ar–^{39}Ar analytical results obtained on basalt flows from the Anjar (Kutch)

Step No.	Atmospheric contamination (%)	^{39}Ar (%)	$^{37}Ar_{Ca}/^{39}Ar_K$	$^{40}Ar^*/^{39}Ar_K$	Age (Ma)
AJ11 whole rock					
1	98.49	0.23	2.576	0.538	15.92 ± 22.87
2	83.30	0.52	3.192	2.039	59.59 ± 9.49
3	43.48	1.03	1.439	2.569	74.76 ± 4.69
4	35.20	2.73	1.087	2.438	71.02 ± 0.50
5	17.42	5.61	1.068	2.402	69.99 ± 0.28
6	7.37	7.08	1.035	2.339	68.20 ± 0.21
7	4.36	9.08	0.965	2.321	67.67 ± 0.16
8	3.69	6.62	0.901	2.295	66.93 ± 0.21
9	3.75	5.40	0.866	2.293	66.87 ± 0.21
10	3.16	6.63	0.832	2.302	67.14 ± 0.16
11	3.31	6.46	0.807	2.298	67.01 ± 0.15
12	3.81	6.27	0.776	2.236	65.24 ± 0.32
13	3.17	4.88	0.696	2.290	66.80 ± 0.16
14	3.16	5.20	0.659	2.287	66.69 ± 0.16
15	2.89	5.63	0.678	2.290	66.79 ± 0.17
16	2.50	2.91	0.751	2.282	66.56 ± 0.26
17	2.81	4.17	1.645	2.285	66.65 ± 0.22
18	2.91	3.72	2.761	2.278	66.45 ± 0.30
19	2.93	15.82	5.088	2.284	66.62 ± 0.39
					Integrated age = 67.10 ± 0.12
AJ11 plagioclase					
1	100.00	0.11	10.256	–	–
2	96.98	0.30	10.433	0.629	18.47 ± 6.03
3	73.10	1.03	12.645	2.015	58.55 ± 1.85
4	72.60	5.18	12.474	2.119	61.52 ± 1.52
5	16.09	7.40	12.550	2.295	66.62 ± 0.94
6	10.67	9.36	12.489	2.284	66.22 ± 0.91
7	9.64	8.97	12.286	2.294	66.51 ± 0.89
8	13.66	4.63	12.050	2.309	66.93 ± 0.91
9	22.17	3.24	11.918	2.287	66.31 ± 1.00
10	21.73	2.34	11.715	2.254	65.37 ± 0.94
11	17.04	4.64	11.770	2.297	66.59 ± 0.92
12	10.99	10.13	12.104	2.306	66.85 ± 0.89
13	13.72	17.38	12.283	2.333	67.62 ± 0.89
14	23.49	11.34	12.324	2.339	67.77 ± 0.91
15	43.55	8.74	12.211	2.344	67.94 ± 0.96
16	72.22	5.20	12.293	2.628	76.00 ± 1.65
					Integrated age = 66.81 ± 0.30
AJ1 whole rock					
1	96.10	0.08	2.584	1.194	35.15 ± 14.43
2	96.43	0.33	3.082	1.178	34.70 ± 6.91
3	87.66	0.63	2.510	2.140	62.51 ± 3.30
4	62.30	0.91	1.973	2.479	72.24 ± 1.50
5	49.13	1.38	1.685	2.442	71.17 ± 1.22
6	41.82	2.66	1.578	2.477	72.18 ± 0.61
7	32.50	5.20	1.770	2.431	70.87 ± 0.40
8	19.68	6.26	2.086	2.380	69.41 ± 0.28
9	11.21	5.92	1.707	2.361	68.85 ± 0.24
10	9.51	6.30	1.310	2.343	68.34 ± 0.25
11	9.34	5.19	1.032	2.335	68.12 ± 0.24
12	8.99	6.00	0.844	2.320	67.69 ± 0.23

Table 2 (*continued*)

Step No.	Atmospheric contamination (%)	^{39}Ar (%)	$^{37}Ar_{Ca}/^{39}Ar_K$	$^{40}Ar^*/^{39}Ar_K$	Age (Ma)
13	6.44	7.57	0.769	2.305	67.27 ± 0.19
14	4.85	6.44	0.881	2.283	66.64 ± 0.17
15	5.99	7.94	1.708	2.249	65.65 ± 0.21
16	6.31	3.12	1.914	2.250	65.70 ± 0.37
17	7.49	10.62	2.764	2.235	65.26 ± 0.32
18	6.89	23.42	4.074	2.237	65.30 ± 0.33
					Integrated age = 67.00 ± 0.11
AJ1 plagioclase					
1	99.19	0.01	71.467	17.748	460.6 ± 351.2
2	85.57	0.28	15.054	2.433	70.53 ± 5.51
3	65.99	3.45	13.953	2.313	67.13 ± 1.65
4	18.65	10.06	13.614	2.275	66.05 ± 1.04
5	14.96	13.65	13.240	2.296	66.64 ± 0.96
6	17.57	10.34	12.821	2.267	65.82 ± 0.97
7	18.17	10.20	12.847	2.283	66.26 ± 0.94
8	17.41	8.97	12.987	2.274	66.02 ± 0.98
9	15.13	15.83	13.083	2.290	66.48 ± 0.96
10	22.83	13.78	13.038	2.293	66.56 ± 0.96
11	56.79	5.00	13.146	2.369	68.72 ± 1.27
12	77.67	2.94	13.230	2.401	69.64 ± 2.03
13	75.29	5.48	12.998	2.391	69.35 ± 1.79
					Integrated age = 66.78 ± 0.34
AJ1 plagioclase					
1	100.0	0.02	23.752	–	–
2	95.39	0.32	10.551	1.933	61.76 ± 7.31
3	68.39	1.56	14.027	2.064	65.89 ± 1.59
4	65.25	8.17	14.002	2.093	66.78 ± 1.42
5	12.40	16.52	13.673	2.085	66.53 ± 1.12
6	13.18	9.50	13.224	2.087	66.61 ± 1.07
7	18.34	6.71	12.933	2.090	66.70 ± 1.03
8	19.47	5.05	12.816	2.086	66.55 ± 1.03
9	14.83	8.02	12.979	2.114	67.46 ± 1.03
10	13.40	8.37	13.257	2.085	66.55 ± 1.06
11	13.43	8.20	13.502	2.106	67.18 ± 1.08
12	17.38	4.60	13.688	2.100	67.02 ± 1.11
13	17.99	6.10	13.798	2.133	68.03 ± 1.11
14	28.75	5.97	13.895	2.119	67.60 ± 1.13
15	27.68	10.90	13.546	2.106	67.20 ± 1.13
					Integrated age = 66.88 ± 0.34
AJ3 whole rock					
1	7.32	0.06	4.555	9.540	263.4 ± 213.4
2	64.06	0.34	4.510	2.957	85.84 ± 39.90
3	12.22	1.53	2.327	2.686	78.14 ± 8.86
4	10.02	5.92	2.188	2.358	68.78 ± 0.40
5	4.01	9.73	1.909	2.310	67.39 ± 0.33
6	1.53	13.45	1.645	2.301	67.13 ± 0.24
7	1.24	18.69	1.343	2.291	66.86 ± 0.18
8	1.04	12.44	1.039	2.294	66.93 ± 0.22
9	1.66	6.90	1.323	2.290	66.84 ± 0.46
10	2.66	3.90	3.070	2.275	66.39 ± 0.64
11	1.26	27.03	8.631	2.286	66.70 ± 0.63
					Integrated age = 67.37 ± 0.30

Table 2 (*continued*)

Step No.	Atmospheric contamination (%)	^{39}Ar (%)	$^{37}Ar_{Ca}/^{39}Ar_K$	$^{40}Ar^*/^{39}Ar_K$	Age (Ma)
AJ4 plagioclase					
1	99.06	0.10	7.512	1.154	33.78 ± 31.83
2	87.12	0.51	14.222	1.986	57.74 ± 3.71
3	68.36	1.62	16.396	2.329	67.55 ± 1.74
4	49.62	5.65	17.336	2.299	66.69 ± 1.42
5	20.48	8.99	17.520	2.247	65.22 ± 1.30
6	15.54	5.18	17.587	2.234	64.82 ± 1.30
7	18.22	5.20	17.567	2.255	65.43 ± 1.33
8	16.56	8.39	17.492	2.253	65.38 ± 1.28
9	12.89	18.73	17.441	2.198	63.82 ± 1.25
10	10.58	17.99	17.444	2.214	64.25 ± 1.25
11	13.67	10.21	17.499	2.264	65.70 ± 1.28
12	9.94	5.75	17.458	2.209	64.11 ± 1.33
13	13.31	2.91	17.432	2.165	62.87 ± 1.48
14	63.62	2.26	17.383	2.485	71.98 ± 1.88
15	33.81	6.52	17.401	2.388	69.22 ± 1.58
					Integrated age = 65.17 ± 0.43
AJ8 whole rock					
1	80.26	0.45	0.350	0.726	21.45 ± 2.78
2	60.32	3.49	0.239	1.125	33.12 ± 0.78
3	40.79	4.01	0.227	1.752	51.30 ± 0.48
4	24.94	5.78	0.302	2.346	68.37 ± 0.37
5	15.05	6.19	0.403	2.511	73.07 ± 0.24
6	12.92	7.11	0.534	2.427	70.69 ± 0.27
7	13.97	6.07	0.720	2.347	68.40 ± 0.32
8	16.78	7.46	0.948	2.291	66.80 ± 0.28
9	15.03	7.80	1.306	2.271	66.21 ± 0.25
10	14.73	9.33	1.476	2.247	65.54 ± 0.23
11	18.39	27.35	2.464	2.228	64.98 ± 0.25
12	17.61	14.96	4.879	2.227	64.96 ± 0.43
					Integrated age = 64.73 ± 0.11

$^{40}Ar^*$ = radiogenic ^{40}Ar; Ca and K: produced by Ca and K neutron interference, respectively. Decay constants are those of Steiger and Jäger [28]. Correction factors for interfering isotopes were $(^{39}Ar–^{37}Ar)_{Ca} = 7.06 \times 10^{-4}$, $(^{36}Ar–^{37}Ar)_{Ca} = 2.79 \times 10^{-4}$, $(^{40}Ar–^{39}Ar)_K = 3.02 \times 10^{-2}$

scope coupled to a PGT X-ray energy dispersive spectrometer. An automatic routine selects particles of the proper density and composition according to specific chemical composition criteria (NiO concentration must be higher than 1% and TiO_2 lower than 1%). The routine allows detection of 1 Ni-rich spinel grain in several thousands of terrestrial magnetic grains. The detection limit depends on the abundance of other magnetic grains, but is generally lower than 0.1 spinel mg^{-1} [18]. Fifteen samples whose Ir content exceeded 0.1 ng g^{-1} were analysed for spinel. Among thousands of terrestrial spinel crystals, we did not find any crystal bearing the characteristic features of K/T Ni-rich magnetite.

4. $^{40}Ar/^{39}Ar$ dating

4.1. Analytical procedure

Minerals were extracted from the bulk basaltic samples. Plagioclase (160–200 μm fraction) were separated using a Frantz magnetic separator, then carefully selected under a binocular microscope, in order to analyse only transparent grains. Whole rocks consist of about 300 μm thick single slabs of rocks. The samples were irradiated in the nuclear reactor at McMaster University in Hamilton, Canada, in position 5c. The total neutron flux density during irradiation was 8.8×10^{18} n cm^{-2}, with a maximum flux gradient estimated

at ±0.2% in the volume where the samples were included. We used the Hb3gr hornblende as a flux monitor, with an age of 1072 Ma ([22], and subsequent analyses in Nice). The plagioclase bulk samples were step-heated with a high frequency furnace, purified in a pyrex line directly connected to a 120°–12 cm MASSE mass spectrometer working with a Baur-Signer source and a Balzers SEV 217 electron multiplier. For single grains and whole rock analyses, the analytical procedures are described in detail by Ruffet et al. [23] and Hofmann [13]. Gas extraction was carried out with a Coherent Innova 70–4 continuous laser; the mass spectrometer is a VG 3600, working with a Daly detector system. The criteria for defining plateau ages were the following: (1) at least 70% (69% for one sample) of released ^{39}Ar, (2) at least three successive steps in the plateau and (3) the integrated age of the plateau should agree with each apparent age of the plateau within a 2σ confidence interval. All uncertainties are quoted at the 2σ level (except the apparent ages in Table 2 and age spectra that are given at the 1σ level) and do not include the uncertainties on the age of the monitor. The uncertainties on the $^{40}Ar^*/^{39}Ar_K$ ratios of the monitor are included in the calculation of the plateau age uncertainty. Detailed analytical data are given in Table 2.

4.2. Results

Three samples were analysed using plagioclase bulk samples (AJ11, 01 and 04) and four using whole rocks (AJ11, 01, 03 and 08). The two samples AJ01 and AJ11 were analysed both as plagioclase and whole rock. Sample AJ01 was duplicated as two plagioclase fractions, irradiated separately, giving concordant plateau ages of 66.9 ± 0.7 and 66.3 ± 0.7 Ma. The four plagioclase samples provide good quality plateau ages ranging from 64.8 ± 0.9 to 67.0 ± 0.6 Ma, corresponding to 88–100% of ^{39}Ar released (Fig. 3). Ages based on $^{36}Ar/^{40}Ar$ versus $^{39}Ar/^{40}Ar$ correlation diagrams (not given) are in all cases in excellent agreement with the plateau ages, though the latter are to be preferred because of the initial $^{36}Ar/^{40}Ar$ ratios (very nearly though not exactly atmospheric). All the age spectra obtained on whole rocks show evidence of ^{39}Ar recoil during irradiation, with high (AJ01, 08) or low (AJ03, 11) disturbances. The less disturbed ones display plateau ages (AJ 03, 11). In the case of AJ11, the plateau age of 66.8 ± 0.3 Ma is in perfect agreement with the plagioclase plateau age. For sample AJ1, the apparent ages converge to a weighted mean age of 65.4 ± 0.4 Ma that is slightly lower than the plagioclase plateau ages, probably due to excess ^{39}Ar in the K-poor phases, such as plagioclase or pyroxene, which degas at high temperatures (as shown by the $^{37}Ar_{Ca}/^{39}Ar_K$ ratio spectrum). On the opposite, whole rock sample AJ08 displays apparent ages converging at high temperatures to a weighted mean age of 65.1 ± 0.4 Ma, that is concordant with the AJ04 plateau age; because of the small Ar fractions (52%) involved, this age can only be considered with great care.

5. Paleomagnetism

5.1. Sampling

As stated in Section 2, each site consists of only one lava flow which moreover generally crops out over only a limited area. This makes accurate measurement of dip difficult, although noticeable dipping (up to 20°) was previously reported in this region [14]. Out of the seven basaltic flows considered by Bhandari et al. [1], only six were sampled, the exposures of flow 'VI' (F8) being judged too bad to obtain reliable results (because of uncertainties in the in situ position of the rocks). Two additional sites (AJ12 and 13) were also sampled in the consolidated sedimentary

→

Fig. 3. $^{40}Ar/^{39}Ar$ age and $^{37}Ar_{Ca}/^{39}Ar_K$ ratio spectra obtained on seven plagioclase bulk samples and whole rocks from basalt flows from the Anjar (Kutch) area (see Fig. 1 for site locations, and Table 1 for correspondence between flow numbers and sample identification. Samples are arranged in stratigraphic order from bottom to top. Uncertainties on apparent ages are given at the 1σ level, whereas plateau ages are given at the 2σ level for comparison with other data.

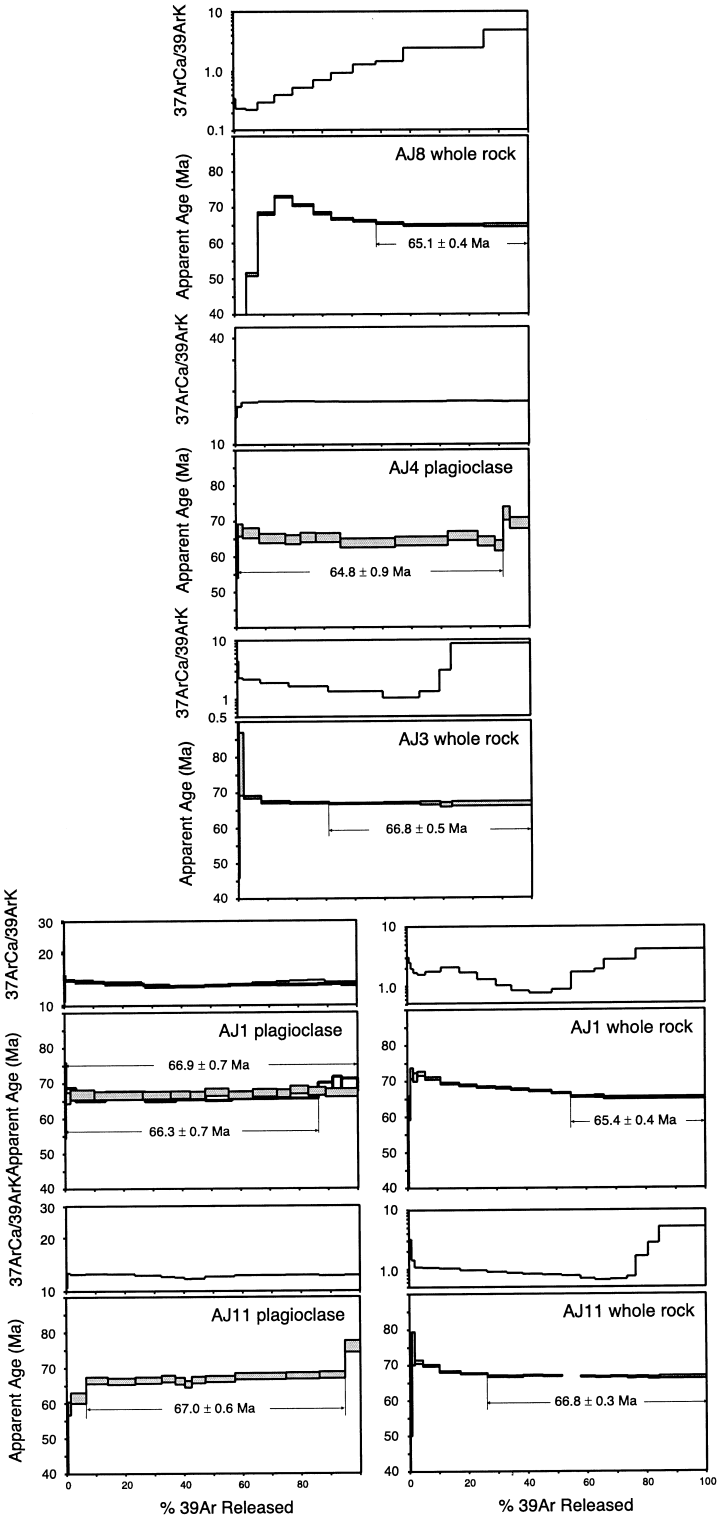
37ArCa/39ArK
Apparent Age (Ma)
AJ8 whole rock
65.1 ± 0.4 Ma
AJ4 plagioclase
64.8 ± 0.9 Ma
AJ3 whole rock
66.8 ± 0.5 Ma
AJ1 plagioclase
66.9 ± 0.7 Ma
66.3 ± 0.7 Ma
AJ1 whole rock
65.4 ± 0.4 Ma
AJ11 plagioclase
67.0 ± 0.6 Ma
AJ11 whole rock
66.8 ± 0.3 Ma
% 39Ar Released
% 39Ar Released

layers (intertrap) deposited below and above the three iridium-rich levels discovered by Bhandari et al. [1]. At each site, a total of 16 cores were collected and the collection was split between the Indian and French groups.

5.2. Analysis

Paleomagnetic analyses of the French collection were carried out in the magnetically shielded laboratory at the Institut de Physique du Globe de Paris. Magnetisation was measured with a JR-5 magnetometer and a 2G cryogenic magnetometer for samples which had been thermally demagnetised and with a 2G cryogenic magnetometer only for samples demagnetised in alternating fields (AF).

The paleomagnetic results show two main sorts of behaviour. The first category concerns sites AJ04, 06, 08 and 10, which correspond to the upper basaltic flows (F4 to F9, excluding F7 and F8). A favourable paleomagnetic behaviour is observed for these sites, which is identical using both demagnetisation techniques (Fig. 4a,b). A soft component is removed in the first demagnetisation steps (up to 200°C or to 10 mT; Fig. 4a,b). This component has roughly the direction of the present day field in the region and is interpreted as a recent viscous magnetisation. At higher temperatures (up to 580°C) and higher fields (up to 100 mT), another component is clearly isolated. The directions obtained for this component are well grouped at the site level (Fig. 5 and Table 3). This component, which is likely carried by a mineral of the magnetite family, has a reversed magnetic polarity for sites AJ04, 06 and 08, and a normal polarity for site AJ10 (considering that India was located in the southern hemisphere).

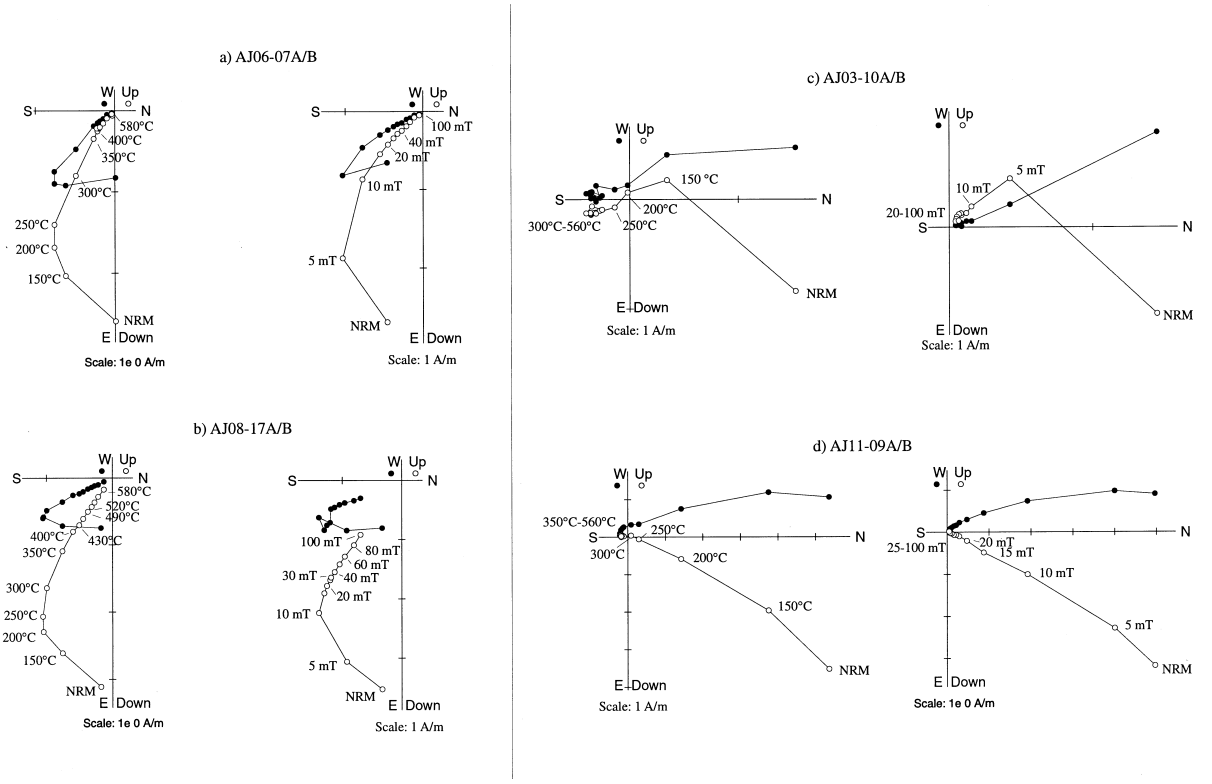

Fig. 4. Examples of AF and TH demagnetisation diagrams for samples from flows F9 (a), F6 (b), F3 (c) and F1 (d). Temperatures in °C and fields in mT. Solid symbols are in the horizontal plane and open symbols in the NS vertical plane. Intensities for space between tick marks on axes are given at the bottom of each diagram in A m^{-1}.

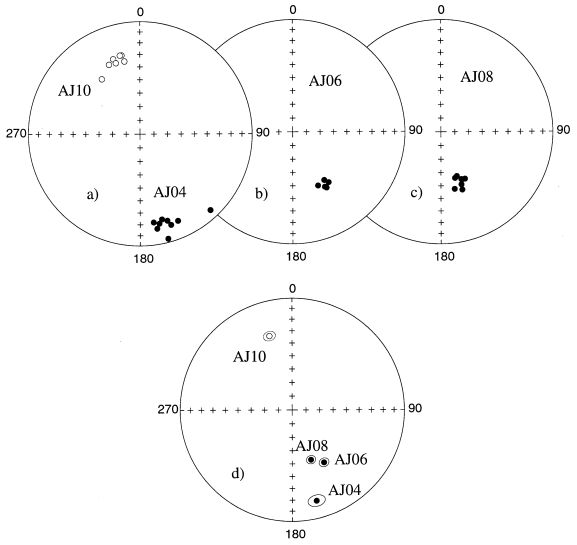

Fig. 5. Equal area projections of paleomagnetic directions isolated within several sites. Closed (respectively open) symbols indicate directions in the lower (respectively upper) hemisphere. The three upper diagrams show directions from all samples from four sites (lava flows): F4 (AJ04), F5 (AJ10), F9 (AJ06) and F6 (AJ08) all above the intertrappean sediments IT3. The lower diagram shows means with α_{95} cones of confidence for the four sites.

Mean directions are given in Table 3. The only problem for these sites results from the different magnetic polarity which is observed for sites AJ04 and AJ10 (Fig. 5), which corresponded to the same lava flow (IV) in the original stratigraphy. On the other hand, Shukla et al. [12] re-interpret these as two separate flows (F4 and F5). This indicates that the chronology of successive flows in Anjar area must be regarded with caution.

The second type of paleomagnetic behaviour is much more problematic and concerns sites AJ01, 02, 03, 09 and 11. If we exclude site AJ09, these sites correspond to the three basaltic flows (F1–F3) from the lower part of the 'Kutch sequence'. This behaviour is characterised by different demagnetisation diagrams when thermal (TH) and AF treatments are considered, although a consistent downward and north directed component is erased in the first demagnetisation steps (Fig. 4c,d). Again, the latter corresponds to a recent viscous magnetisation. After removal of this component, the demagnetisation results become very different. When the samples are AF demagnetised, a component going to the origin is isolated up to 100 mT. This component has a normal polarity assuming acquisition in the southern hemisphere. In contrast, when the samples are thermally demagnetised, a similar component is obtained up to $\sim$350°C, but only as an intermediate one, masking a higher temperature (above $\sim$500°C) component of opposite polarity (Fig. 4c,d). This high-temperature component is obvious in most samples, although the overlap between the intermediate and final components varies, depending on the samples and/or the sites. No precise direc-

Table 3
Paleomagnetic mean directions obtained from Anjar basalt flows (F) and intertrappean sediments (IT3)

Lava flows/sediments	Paleomagnetic sites	Demagnetisation treatment	N	Declination	Inclination	α_{95}	K
F9	AJ06	Th+AF	5	149.0°	41.8°	3.6°	442.6
F8	–		–	–	–	–	–
F7	AJ09	x	x	x	x	x	x
F6	AJ08	Th+AF	7	159.2°	50.9°	2.6°	381.2
F5	AJ10	Th+AF	6	343.6°	−30.6°	3.8°	311.2
F4	AJ04	Th+AF	8	164.7°	18.1°	4.2°	172.3
IT-3	AJ12	x	x	x	x	x	x
IT-3	AJ13	Th+AF	3	330.5°	−26.4	17.3°	52.1
F3	AJ02	AF	7	326.6°	−55.8°	6.6°	83.4
F3	AJ03	AF	6	353.7°	−47.8°	13.3°	26.2
F2	AJ01	AF	8	309.7°	−24.0°	9.5°	35.1
F1	AJ11	AF	7	322.5°	−2.9°	12.2°	25.3

Columns give lava flow code, sample code, demagnetisation treatment (AF = alternating field, TH = thermal), number of specimens used in the mean, mean declination (in °), inclination (in °), α_{95} confidence interval and kappa (Fisher's precision parameter K).

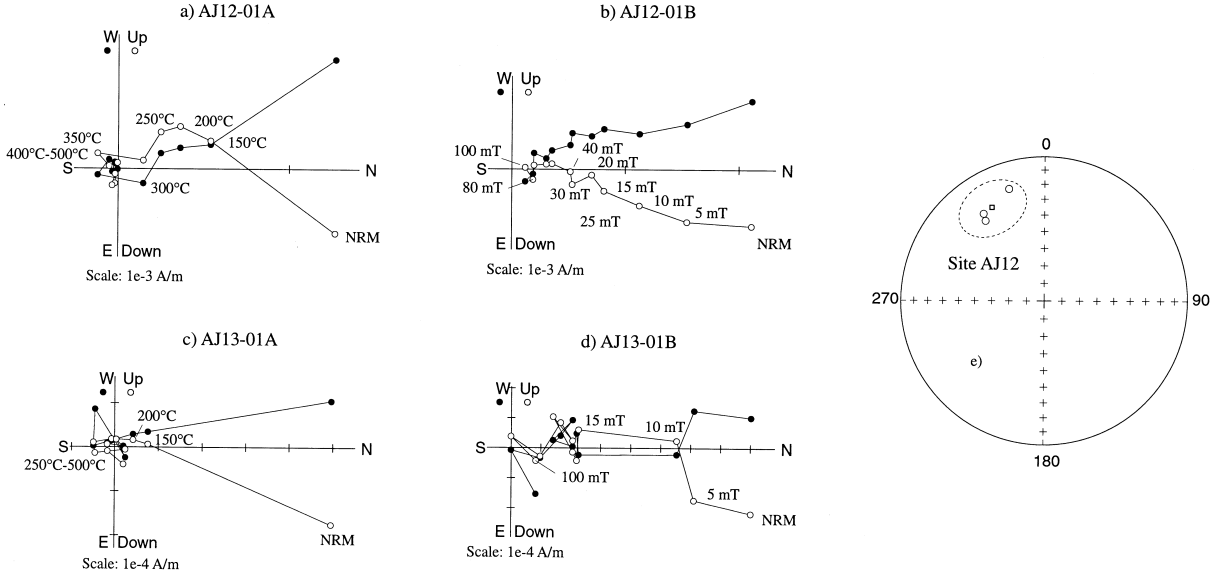

Fig. 6. Examples of AF and TH demagnetisation diagrams for samples from intertrappean sediments below (AJ12) and above (AJ13) the iridium levels. See caption of Fig. 4 for specifications. An equal area projection for the three samples for which a clear magnetic component could be isolated is shown at the right of the figure.

tions can be obtained for several reasons. One is the large overlap between the demagnetisation spectra of the intermediate and high temperature components. Another is due to the high magnetic viscosity of these samples which prevents a clear end of demagnetisation. The last reason is fortuitous and very unfortunate, since we detected a spurious magnetic field of about 1000 nT amplitude in the cooling part of the oven after some of our experiments. However, further experiments on our very few remaining samples in an oven whose internal magnetic field is less than 20 nT confirmed the above observations. Due to these problems, TH demagnetisations cannot be considered as definite proof for the existence of a consistent magnetic component above 580°C. Isothermal remanent magnetisation experiments carried out on several samples for each site show in all cases a saturation in fields of $\sim$0.15 T and no difference in behaviour is observed between the two groups of sites. That a small fraction of hematite (and/or some maghemite) could carry the reversed component found in sites of the second group is therefore not demonstrated. Yet, this would have major importance to constrain the timing of acquisition of this component.

We also present the paleomagnetic results from the two sedimentary beds below and above the Ir-rich layers (Fig. 6). The demagnetisation data are very scattered and make it difficult to determine a clear characteristic component. This problem is even more important for site AJ13, for which no reliable component can be isolated (Fig. 6). Site AJ12 seems more interesting, because in some samples both TH and AF demagnetisations yield a consistent north-west and upward directed component (Fig. 6). A mean direction with a normal polarity is estimated from three cores (corresponding to five specimens), though some indications of an underlying reversed component, similar to that established in the lava flows of Fig. 4c,d, cannot be excluded. However, we insist on the poor quality of these data as shown by Fig. 6, and on the small number of directions used for the site mean computation.

6. Discussion

The most likely explanation for the high iridium concentrations observed in the Anjar intertrappean sediments is that they are in some way

related to the K/T impact and hence correspond or are close to the stratigraphic K/T boundary. That these sediments do correspond to the boundary and are in place [1,2] would seem to be in agreement with earlier reports that the last dinosaur remains occur below the sediments. The local existence of multiple Ir-rich levels is an important observation which does not necessarily imply that multiple collisional events occurred at the K/T boundary: the observed multiplicity could indeed have resulted from redeposition effects.

Bajpai [4] uncovered fossiliferous sediments from fresh excavations near the original iridium site, yielding 'abundant dinosaur (ornithoid) eggshells identical to those found between the middle and upper iridium levels', yet above the uppermost iridium level. However, correlation between his section and our section has not been established. More recently, Bajpai and Prasad [5] have described the occurrence of theropod eggshell fragments together with late Cretaceous ostracods above the upper iridium level. Moreover, they note the absence of any exclusively Paleocene taxa, and believe that there was only minor later mechanical reworking. This would place all of the Ir-bearing sediments within the uppermost Maastrichtian, prior to but not at K/T time.

The absence of Ni-rich spinel suggests that the lowermost K/T clay layer is not present at Anjar. This is not necessarily surprising in view of the lines of evidence which indicate that this section may be disturbed and probably incomplete (viz. the multiple and relatively low Ir anomalies, as far as K/T anomalies go, strong horizontal variations in the stratigraphical extent of the geological units, and possibly the paleontological observations of [4,5]). The absence of spinels at Stevns Klint (Denmark), a section where a hiatus might exist at the top of the Cretaceous [24,25], has been noted. We must keep in mind that K/T spinel crystals, unlike Ir, are not uniformly distributed at a global scale. In several continuous K/T sites, Ni-rich spinel crystals are rare (for instance at Mimbral in Mexico [26]). Finding this mineral in the Anjar intertrap would have firmly established a causal link between the Ir anomalies and the K/T event but the absence of this mineral leaves the question open.

The Ir data do suggest that the Anjar intertrap contains some imprint of the K/T boundary event, since such anomalous concentrations within uppermost Maastrichtian to K/T sediments are unlikely to be due to terrestrial processes and are believed to provide evidence for the impact. Because the observations of Bajpai and Prasad [5] argue against significant mechanical reworking, a likely explanation is that the observed lacustrine sediments were indeed entirely emplaced within the uppermost Maastrichtian, prior to K/T time, that the impact signatures were deposited on top of those, and that further chemical and fluid alteration, most likely following emplacement of the F4 flow, led to downward redistribution of the iridium, which became enriched at several distinct levels and locations in a heterogeneous, nonuniform fashion. This interpretation is consistent

Table 4
^{40}Ar–^{39}Ar plateau ages and correlation diagram data obtained on basalt flows from Anjar (Kutch)

Section	Sample No.	Plateau age (Ma)	Weighted mean age (Ma)	^{39}Ar (%)	Isochron age (Ma)	$(^{40}Ar/^{36}Ar)_i$	MSWD
Upper part	AJ8 w.r.	–	65.1 ± 0.4 (10–12)	52	–	–	–
	AJ4 plag.	**64.8 ± 0.9** (3–13)	–	91	**64.6 ± 0.8** (3–13)	303.4 ± 3.2	0.2
Lower part	AJ3 w.r.	**66.8 ± 0.5** (7–11)	–	69	–	–	–
	AJ1 plag.	**66.3 ± 0.7** (3–10)	–	86	**66.3 ± 0.7** (1–13)	299.4 ± 1.2	0.3
		66.9 ± 0.7 (3–15)	–	100	**67.2 ± 0.4** (1–15)	292.6 ± 1.9	1.3
	AJ1 w.r.	–	65.4 ± 0.4 (15–18)	45	–	–	–
	AJ11 plag.	**67.0 ± 0.6** (5–15)	–	88	**66.3 ± 1.0** (5–15)	304.4 ± 10.2	0.6
	AJ11 w.r.	**66.8 ± 0.3** (8–19)	–	74	–	–	–

The part of the section, sample number (plag. = plagioclase separate, w.r. = whole rock), plateau age (in Ma, with 2σ uncertainty, with temperature steps used), weighted mean age (with steps), percent of ^{39}Ar in the steps used in the plateau, isochron age (with steps), initial ratio from correlation diagram plot, and mean standard weighted deviation are given in columns from left to right

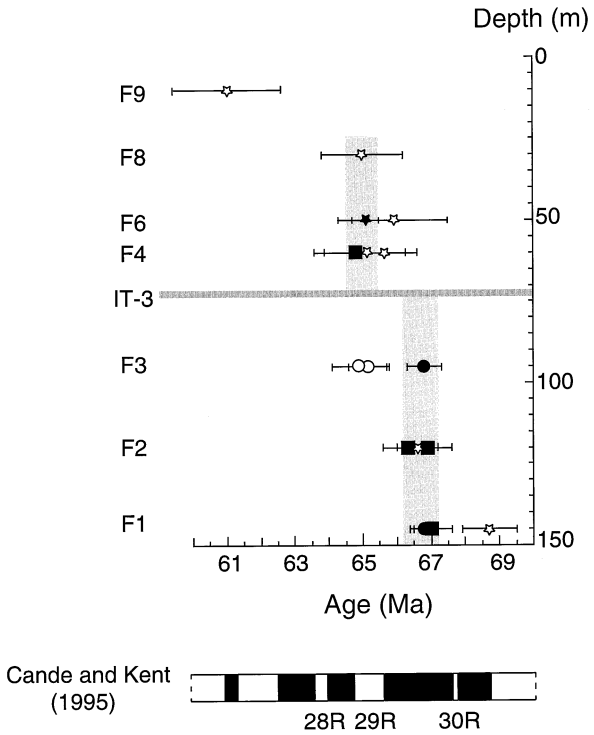

Fig. 7. $^{40}Ar/^{39}Ar$ ages versus stratigraphic position for the Anjar flows. The ages determined in this paper are shown as solid symbols, the ages determined by Venkatesan et al. [11] and listed by Shukla et al. [12] are shown as open symbols. Squares denote a plateau age on a plagioclase sample, circles a plateau age on a whole rock sample, and stars an integrated (or weighed mean, or low quality plateau) age on a whole rock sample. The shaded vertical bars correspond to our preferred interpretation of the two relatively short and separate phases of volcanism at Anjar. See Tables 2 and 4 for numerical results.

with the absence of Ni-rich spinel, a mineral which, unlike iridium, cannot be redistributed after deposition by chemical processes [15,18]. Available data about cosmic markers therefore lead us to consider that the K/T impact event was recorded, but under unfavourable conditions. Alternative interpretations that (1) the Ir anomalies correspond to multiple intra-Maastrichtian events, or (2) dinosaurs and other Maastrichtian taxa found by [4,5] survived the impact, are considered unlikely and cannot be considered unless the simpler solution we propose (in an application of Occam's razor) is shown to be untenable for as yet unknown reasons.

As far as our $^{40}Ar/^{39}Ar$ age determinations are concerned, companion samples collected from the same flows at the same sites have been dated independently by Venkatesan et al. [11] (Table 4 and Fig. 7; as quoted by Shukla et al. [12]). More precisely, Venkatesan et al. [11] report results from flows F3 and F4 (two spectra from two samples each) only, whereas Shukla et al. [12] report eight ages which they assign to the same reference [11]. The ages not published in [11] were actually reported in a preprint and as an oral communication provided by the authors. In order to avoid confusion, we refer to the results as listed most recently by Shukla et al. [12] in their Table 1, and also to the spectra shown by Venkatesan et al. [11] as their Fig. 2. All are whole rock samples, some having yielded plateau ages (F1, F2, F3 and F9, the last one with a large uncertainty), the others not (only integrated ages: F4, F6 and F8). In two cases, the agreement between the two independent sets of ages is good (F2 and F4), although the two ages reported in [11,12] are different. Actually, the two samples from flow F4 determined by [11] display disturbed age spectra,

characteristic of strong ^{39}Ar recoil. The authors nevertheless propose an age of 65.7 ± 0.7 Ma at intermediate temperatures, which is concordant with our plateau age obtained on a plagioclase (AJ4) from the same lava flow. In one case (F6 = AJ08) there is good agreement, but we do not obtain a plateau age on whole rock, only a much less reliable weighted mean age; and in two cases there is significant discrepancy: for F1 (= AJ11), the difference is 1.7 ± 1.0 (2σ) Ma and for F3 (= AJ3), 1.6 ± 0.8 (2σ) Ma. The sign of this difference changes, with the oldest (respectively youngest) age from Venkatesan et al. [11] being older (respectively younger) than the one which we obtain. When the two sets of results are plotted in stratigraphic order (Fig. 7), two different pictures emerge. For Venkatesan et al. [11], the three lower flows decrease regularly in age upwards from 68.7 to $\sim$65 Ma (covering a range of 3.8 ± 1.3 (2σ) Ma), whereas the lava flow just below and the flows above the iridium-bearing intertrappean sediments have a similar age near 65 Ma. Our data would rather indicate that the three lower flows are roughly coeval at $\sim$66.5/67 Ma, with those above the iridium-bearing levels identical to those of Venkatesan et al. [11]. Note that our ages are based on concordant plateau ages from plagioclase separates, whereas those from Venkatesan et al. [11] are based on plateau ages and weighted mean ages on whole rocks. It is therefore worth discussing further, possible reasons for these discrepant results. In a separate paper on $^{40}Ar/^{39}Ar$ measurements from the Deccan traps [3], we point out a number of problems with $^{40}Ar/^{39}Ar$ ages, even plateau ages, when they are based on whole rock samples only, since additional effects of alteration and recoil of ^{39}Ar may remain hidden. We conclude that it is safer, whenever possible, to rely on plateau ages for mineral separates. This would argue in favour of the Kutch lava flows representing two separate volcanic events of short duration, one at $\sim$66.5–67 Ma, the other at $\sim$65 Ma, with a $\sim$1.5 Ma gap between the two. This leaves the age of the sedimentary layer ill-constrained.

The interpretation of the paleomagnetic data that we obtain from the Kutch region is difficult for two reasons. One is due to the lack of good stratigraphic constraints in the area. As a consequence, the chronology of basaltic flows proposed by Ghevariya [14] could, as already pointed out, in part be erroneous (see in particular the different polarities of sites AJ04 and AJ10). However, the two very distinct types of paleomagnetic behaviour that we observe in our study can be used to distinguish two groups of sites, which could have erupted at different times: these two groups indeed constitute, respectively, the lower and upper parts of the sequence, separated by the iridium-bearing sediments. The second difficulty is due to the paleomagnetic behaviour observed in several sites. Whereas those sites from the upper part of the sequence are clearly of reversed magnetic polarity (assuming of course that the magnetisation was acquired during trap emplacement, which is supported by magnetic analyses), the sites from the lower part of the sequence yield two components with opposite polarities. The first has normal polarity and is isolated by AF demagnetisation; it is likely carried by magnetite. The second component with reversed polarity has a high blocking temperature range above 560°C and could be carried by magnetite, maghemite or possibly hematite. If the component with reversed polarity is carried by maghemite or hematite, we propose that it was acquired due to alteration, probably linked with emplacement of the overlying reversed flows, after the original component with normal polarity carried by magnetite. Following this scheme, the lower part of the sequence would have a 'primary' normal polarity and the upper part of the sequence a 'primary' reversed polarity. The change in polarity would then coincide with the intertrappean sediments, between flows F3 and F4, containing the Ir-enriched layers. Site AJ12, located in these sediments below the Ir layer, apparently has a normal polarity, which may agree with the polarity of the underlying lava flows, but then cannot be of K/T age (in agreement with the paleontological observations of [4,5]). Site AJ13 unfortunately does not provide any reliable paleomagnetic results, which could have better constrained the link between the Ir layers and the K/T boundary. But, again, we

wish to emphasise that the paleomagnetic results obtained on these sediments do not allow any firm conclusion to be drawn.

The scenario would be drastically different if one would assume that the reversed polarity component in the lower lava flows is primary and that the normal polarity component was acquired more recently (though it must be an ancient component, acquired prior to the time when the site passed the equator, i.e. ~50 Myr ago). In this case, all the Kutch sequence could have been erupted during a reversed polarity chron which could then only have been C29R. The situation would have been obscured later because of the magnetic properties (in particular the higher viscosity found during thermal treatment) of the lava flows belonging to the second group.

This scenario is challenged by our own $^{40}Ar/^{39}Ar$ data, where we consider the ~66.5/67 Ma age for the three lava flows as reliable. The paleomagnetic data reported by Hofmann [13] were preliminary and are superceded by the present report. There is overall agreement from all groups and laboratories on the reversed polarity of upper flows F4, F6 and F8. There is also agreement on the normal polarity of F5, which does not fit the picture and because of the concordant ages of the surrounding flows cannot be coeval. There is no doubt that F4, F6 and F8 were emplaced in a relatively short period of time around 65 Ma within reversed chron C29R [27], somewhat after K/T boundary time, as defined by the iridium-bearing sediments. F5 could be a later dyke emplaced after the end of C29R. Indeed, the site is located very close to a dyke mapped in Fig. 1 (note however that one of us, Z.G.G., is not of that opinion).

Note that the mean paleomagnetic poles for, respectively, the four lava flows above the Ir-layers and the five lava flows below are statistically indistinguishable ($\lambda = 42.0°N$, $\Phi = 276.5°E$; $A_{95} = 13.4°$; versus $\lambda = 37.5°N$, $\Phi = 289.1°E$; $A_{95} = 19.8°$). This would argue against the normal magnetisation of the five lava flows having a recent viscous origin. The 95% confidence intervals are of course quite large because of the small number of sites; also for the same reason, secular variation may not have been averaged out. These two results, and even better, the overall mean ($\lambda = 39.7°N$, $\Phi = 283.6°E$; $A_{95} = 11.0°$; $N = 9$) are compatible with the Deccan trap pole of Vandamme et al. [8] ($\lambda = 36.9°N$, $\Phi = 281.3°E$; $A_{95} = 2.4°$).

On the other hand, the age progression proposed by Venkatesan et al. [11] for the lower lava flows, which relies on whole rock measurements, though not inconsistent with the magnetic polarities obtained by Shukla et al. [12] (F1 remagnetised, F2 and F3 normal, no reversed overprint observed), does not lead to a compelling scenario. Our own age determinations, all based on concordant plagioclase plateau ages, and magnetic polarities are consistent with a simple scenario of a rather short volcanic episode for the lower flows within normal chron C30N [27].

7. Conclusion

In conclusion, pending further detailed geological fieldwork, most notably on the validity of the Kutch stratigraphy [12,14], we believe that the following scenario, though certainly non-unique, is the simplest one fitting available observations, including the most recent described in the present paper.

An early phase of Deccan trap volcanism occurred near 66.5–67 Ma (F1, F2, F3), most likely within magnetic normal chron C30N [27] in the Kutch area. This is on the early side compared to ages found in the main part of the province, notably along the thick Mahabaleshwar section [3,7,8], though it is consistent with the idea that volcanism did not start prior to C30N. Note that this may have involved only a very small volume of lava. Volcanism would have stopped locally in Kutch for 1 to 2 Ma, when uppermost Maastrichtian lacustrine sediments were deposited. These sediments, which have apparently not been significantly reworked mechanically [4,5], bear witness to the K/T impact (within C29R) in the form of anomalous but redistributed iridium concentrations, but with no other cosmic marker such as Ni-rich spinels. Shortly following this, and still within chron C29R, volcanism resumed in Kutch as witnessed by a series of reversed flows

near 65 Ma in age (F4, F6, F8). At that time, the underlying normal flows suffered some amount of reversed remagnetisation and the sediments were altered: most notably, the iridium from the topmost sediments was redistributed, probably through fluid flow, in the layers below. Evidence for minor later volcanism is attested by a normal crosscutting dyke (F5); the last flow (F9) at 61 ± 1.6 Ma has a very perturbed spectrum and a large uncertainty and is of little value [11]. This scenario does not contradict the occurrence of Deccan trap volcanism within a series of three chrons (C30N, C29R and C29N [3,6–8]), with most of the volume erupted within a period of less than 1 Ma (much of this in reversed chron C29R which contains the K/T boundary). The Kutch sequence provides evidence for minor (?) volumes at an early time (up to 67 Ma). But the image of regular long lasting volcanism is not supported (see [3]). The main finding of Bhandari et al. [1] that Deccan volcanism and K/T bolide impact were both recorded in India, and could be shown to have occurred at the same general time (though not the same time scales), without any causal connection, is basically vindicated. In closing, we should recall the difficulties encountered in obtaining accurate mapping, stratigraphic placement, reliable age determinations or identification of primary paleomagnetic components in several flows. There is therefore ample room for further work on these fascinating outcrops.

Acknowledgements

We thank F. Asaro and an anonymous reviewer for useful comments. French scientists wish to thank the staff of PRL for their warm welcome and help in the field. This work was supported by the IPGP BQR (Bonus Qualité Recherche) science program. IPGP contribution No. 1700.*[AC]*

References

[1] N. Bhandari, P.N. Shukla, Z.G. Ghevariya, S. Sundaram, Impact did not trigger Deccan volcanism: evidence from Anjar K/T boundary intertrappean sediments, Geophys. Res. Lett. 22 (1995) 433–436.

[2] N. Bhandari, P.N. Shukla, Z.G. Ghevariya, S. Sundaram, K/T boundary layer in Deccan intertrappeans at Anjar, Kutch, Geol. Soc. Am. Spec. Pap. 307 (1996) 417–424.

[3] C. Hofmann, G. Féraud, V. Courtillot, $^{40}Ar/^{39}Ar$ dating of mineral separates and whole rocks from the Western Ghats lava pile: further constraints on duration and age of the Deccan traps, Earth Planet. Sci. Lett. 180 (2000) 13–28.

[4] S. Bajpai, Iridium anomaly in Anjar Intertrappean beds and the K/T boundary, Geol. Soc. India Mem. 37 (1996) 313–319.

[5] S. Bajpai, G.V.R. Prasad, Cretaceous age for Ir-rich Deccan intertrappean deposits: paleontological evidence from Anjar, western India, J. Geol. Soc. London 157 (2000) 257–260.

[6] V. Courtillot, Evolutionary Catastrophes: the Science of Mass Extinctions, Cambridge University Press, 1999.

[7] V. Courtillot, J. Besse, D. Vandamme, R. Montigny, J.J. Jaeger, H. Cappetta, Deccan flood basalts at the Cretaceous/Tertiary boundary?, Earth Planet. Sci. Lett. 80 (1986) 361–374.

[8] D. Vandamme, V. Courtillot, J. Besse, R. Montigny, Paleomagnetism and age determinations of the Deccan traps (India): results of a Nagpur-Bombay traverse and review of earlier work, Rev. Geophys. 29 (1991) 159–190.

[9] L.W. Alvarez, W. Alvarez, F. Asaro, H.V. Michel, Extraterrestrial cause of the Cretaceous/Tertiary extinction, Science 208 (1980) 1095–1108.

[10] W. Alvarez, T. rex and the Crater of Doom, Princeton University Press, Princeton, NJ, 1997.

[11] T.R. Venkatesan, K. Pande, Z.G. Ghevariya, ^{40}Ar–^{39}Ar ages of the Anjar traps, western Deccan province (India) and its relation to the Cretaceous-Tertiary boundary event, Curr. Sci. 70 (1996) 990–996.

[12] A.D. Shukla, N. Bhandari, S.C. Chakraborty, S. Kusumgar, P.N. Shukla, Z.G. Ghevariya, V. Balaram, Deccan trap alkali basalts of Anjar, Kutch, and their relation to the K/T boundary and the Reunion plume, Earth Planet. Sci., Proc. Indian Acad. Sci. (2000) in press.

[13] C. Hofmann, Datation $^{40}Ar/^{39}Ar$ et paléomagnétisme des traps d'Ethiopie, du Deccan et de Sibérie, Ph.D. thesis, Université Paris 7-IPGP, 1997.

[14] Z.G. Ghevariya, Intertrappean dinausorian fossils from Anjar area, Kutch district, Gujarat, Curr. Sci. 57 (1988) 248–251.

[15] E. Robin, Ph. Bonté, L. Froget, C. Jéhanno, R. Rocchia, Formation of spinels in cosmic objects during atmospheric entry: a clue to the Cretaceous-Tertiary boundary event, Earth Planet. Sci. Lett. 108 (1992) 181–190.

[16] J. Smit, F.T. Kyte, Siderophile-rich magnetic spheroids from the Cretaceous-Tertiary boundary in Umbria, Italy, Nature 310 (1984) 403–405.

[17] F.T. Kyte, J. Smit, Regional variations in spinel compositions an important key to the Cretaceous-Tertiary event, Geology 14 (1986) 485–487.

[18] E. Robin, D. Boclet, Ph. Bonté, L. Froget, C. Jéhanno, R. Rocchia, The stratigraphic distribution of Ni-rich spinels in Cretaceous-Tertiary boundary rocks at El Kef (Tunisia), Caravaca (Spain) and Hole 761C (Leg 122), Earth Planet. Sci. Lett. 107 (1991) 715–721.

[19] E. Robin, R. Rocchia, Le spinelle nickélifère de la limite Crétacé-Tertiaire du site d'El Kef, Tunisie, Bull. Soc. Géol. Fr. 169 (1998) 365–372.

[20] G. Meyer, Multiparameter coincidence spectrometry applied to the instrumental neutron activation analysis of rocks and minerals, J. Radioanal. Nucl. Chem. 114 (1987) 223–230.

[21] G. Meyer, D. Piccot, R. Rocchia, J.P. Toutain, Simultaneous determination of Ir and Se in K–T boundary clays and volcanic sublimates, J. Radioanal. Nucl. Chem. 168 (1993) 125–131.

[22] G. Turner, J.C. Huneke, F.A. Podose, G.J. Wasserburg, ^{40}Ar–^{39}Ar ages and cosmic ray exposure ages of Appolo 14 samples, Earth Planet. Sci. Lett. 12 (1971) 19–35.

[23] G. Ruffet, G. Féraud, M. Amouric, Comparison of ^{40}Ar–^{39}Ar conventional and laser dating of biotites from the North Trégor Batholith, Geochim. Cosmochim. Acta 55 (1991) 1675–1680.

[24] K. Perch-Nielsen, Cretaceous nannofossils at the Cretaceous-Tertiary boundary near Biarritz, France, in: W. Christensen, T. Birkelund (Eds.), Cretaceous-Tertiary Boundary Events, Copenhagen University 2, 1979, pp. 151–155.

[25] K. Perch-Nielsen, J. McKenzie, Q. He, Biostratigraphy and isotope stratigraphy and the 'catastrophic' extinction of calcareous nannoplankton at the Cretaceous-Tertiary boundary, in: L. Silver, P. Schutz (Eds.), Geological Implications of Impacts of Large Asteroids and Comets on the Earth, Geological Society of America Special Paper 190, 1982, pp. 353–371.

[26] R. Rocchia, E. Robin, L. Froget, J. Gayraud, Stratigraphic distribution of extraterrestrial markers at the Cretaceous-Tertiary boundary in the Gulf, in: S. Gartner (Ed.), The Cretaceous-Tertiary Event and other Catastrophes in Earth History, Geological Society of America Special Paper 307, 1996, pp. 279–286.

[27] S.C. Cande, D.V. Kent, Revised calibration of the geomagnetic polarity time scale for the late Cretaceous and Cenozoic, J. Geophys. Res. 100 (1995) 6093–6095.

[28] R.H. Steiger, E. Jäger, Subcommission on geochronology: convention of the use of decay constants in geo- and cosmochronology, Earth Planet. Sci. Lett. 36 (1977) 359–362.